EXTRACTION OF MINERAL ALTERATION ANOMALY ZONE FROM ASTER DATA IN MANZHOULI, CHINA

Zhaoqiang Huang

Institute of Mineral Resources, China Metallurgic Geology Bureau, 105 Yaojiayuan Road, Beijing, P.R. China, 100025

1. INTRODUCTION

All sorts of anomaly graphs of physical geography and geochemistry, such as aeromagnetic anomaly graphs, bouguer gravity anomaly graphs, regional geochemical anomaly graphs and so on, are all parameters for exploration deposit. And following the remote sensing image shortwave and infrared bands coming, researchers of remote sense have engaged in many highly effective experiments and have approved that there are high relativity between altered rocks information and metal deposit. So hydrothermal alteration information extracted from remote sense information can be as an important exploration mine sign.

The Advanced Spaceborne Thermal Emission and Reflection Radiometer (ASTER) is an advanced multispectral imager and covers a wide spectral region with 14 bands, which are 3 bands between 0.52 and 0.85 μm, 6 bands from 1.6 to 2.43 μm and 5 bands in the 8.125- to 11.65-μm wavelength region with 15-m, 30-m and 90-m resolution respectively, from visible to thermal infrared with high spatial, spectral, and radiometric resolution [1]. The VNIR, SWIR and TIR wavelength regions provide complementary data for lithologic mapping [2] and geological application [3].

The Manzhouli area, Inner Mongolia in China mineralized study area, is underlain by a hydrothermally altered rocks zone associated with Ag-Pb-Zn deposits mineralization. The purpose of this study was to evaluate ASTER data acquired on August 22, 2004, for recognizing and extracting alteration anomaly zones in the study area. The paper firstly discusses the spectral features discernable in laboratory and field spectra of the Orefield spectra convolved to ASTER spectral resolution. And then the relationship between lithologic composition and spectral features of the field samples is founded. Following above, hydrothermally altered rocks classification are analyzed based on use of the ASTER image data.

2. GEOLOGIC SETTING

The Manzhouli area，Inner Mongolia, China, is an important metallogenic province of nonferrous and noble metals. The regional strata consist mainly of Mesozoic continental volcano-sedimentary formations. And the Jiawula, Chiaganbulagen and Eren Tolgoi Ag-(Pb-Zn) deposits occur on the bottom of the strata. The geotecture place of the area locates in the Southeast exterior edge of Siberian Platform. And there are a series of volcanic rocks and the pyroclastic rocks, volcanoclastic rock, clastic rocks. It is the mainly horizon that many polymetallic mines deposit. Moreover, magmatic activity of the area is frequency. The main faulted structure in the area is northeast Erguna-HunLunbeier deep faulted belt which is a supracrustal deep fault that controls the volcanic magmatic activity and facilitates the deep crustal minerals upwelling. Gradually, minerals deposit in the feasible uplifted structure.

3. ASTER SPECTRAL PROPERTIES AND IMAGE ANALYSIS

3.1. Spectral properties

Analysis of ASTER data for extracting alteration anomaly zones is based on determination of the relationship between spectral reflectance and spectral emittance and the mineral composition of the rocks units of interest [4]. Spectral reflectance measurements of the field samples were made in situ during September 2009 using a Spectra Vista Corporation (SVC) field-portable spectroradiometer, which records 1024 channels throughout the 350nm to 2500nmwavelength region, and then resampled to the 9 VNIR and SWIR ASTER bandpasses. Reflectance spectra ware obtained from the 40 samples collected in the study area.

Representative visible and near-infrared laboratory reflectance spectra of the samples collected at the study area were characterized by absorption features that indicate the presence of silicic, phyllic, argillic and propylitic alteration minerals, including quartz, K-Feldspar, muscovite, chlorite, calcite, illite, and epidote.

A laboratory reflectance spectrum representing phyllic altered rock from the study area exhibits absorption features of typical minerals of phyllic alteration. Phyllic alteration of feldspars produces Al-phyllosilicate minerals, such as muscovite, whose spectra has an instense Al-OH absorption feature near $2.20\,\mu m$ which locates at the 6 band of ASTER and secondary features near 2.35 and $2.44\,\mu m$ which locate at the 8 band of ASTER, and an O-H feature near $1.40\,\mu m$. The $1.40\,\mu m$ feature is not useful for analyzing remotely sensed data, as it is obscured by atmospheric absorption [5]. The spectral absorption features exhibited in a propylitized altered granitoid sample indicate an assemblage of chlorite and muscovite. Chlorite is responsible for the main Fe,Mg－OH absorption feature near $2.35\,\mu m$ which locates on the 8 band of ASTER and the secondary feature at 2.25 μm, as well as the multiple broad ferrous-iron features located in wavelength region short of $1.3\,\mu m$. Some of the sample spectra exhibit ferriciron features near $0.92\ \mu m$ and at $0.43\ \mu m$.

ASTER bands 1 through 9 were used for all the endmembers because of importance of ferric- and ferrous-iron absorption, as well as the concentration of spectral absorption features in the 2.1 to $2.45\,\mu m$ wavelength region.

3.2. Extraction of mineral alteration

The ASTER band ratio 4/3 was applied to differentiate vegetation. Areas where the band ratio 4/3 was less than 0.3 were regarded as densely vegetated and masked. And the processing of internal average reflectance (IAR) can also eliminate the some effects of atmosphere and cloud.

Principal component analysis (PCA) is an orthogonal transformation of the uncorrelated linear combinations (eigenvector loadings). This method may retain the characteristics of multispectral data, which contribute most to its variance. In this study, PCA was employed to process ASTER bands. Given the diagnostic features of the mineral alterations, the mineral alteration component in the PCs may gain positive contributions from bands, which have high reflectance of mineral alteration. Furthermore, the alteration component may also obtain a negative contribution from the band, which has high absorption of mineral alteration [6].

The PCA of ASTER bands 1, 3, 4, and 6 was adopted to extract areas of Al-OH alteration. This extraction was done because the Al-OH ion has high reflectance in band 4 and high absorption in band 6. Consequently, four principal components (PCs) were obtained, and the loadings are shown in Table 1. Similarly, the PCA of ASTER bands 1, 3, 4, and 8 was used to extract Fe/Mg-OH alteration. Four PCs were obtained for Fe/Mg-OH ions and are shown in Table 2. And the PCA of ASTER bands 1, 2, 3, and 4 was used to extract Fe^{2+} and Fe^{3+} ions. This processing is based on the principle that Fe^{2+} and Fe^{3+} ions have high absorption in band 3 and in band 1. Four PCs were obtained for Fe^{2+} and Fe^{3+} ions and are shown in Table 3.

Table 1 Principal components from ASTER bands1, 3, 4, and 6 for Al-OH alteration

PCs	Channel				V（%）
	ASTER1	ASTER3	ASTER4	ASTER6	
PC1	0.79399	0.59177	0.13511	0.03360	92.13%
PC2	0.60628	-0.75398	-0.24675	-0.05532	6.25%
PC3	0.04454	-0.28495	0.92315	0.25417	1.60%
PC4	-0.00462	0.01122	-0.26200	0.96499	0.03%

Table 2 Principal components from ASTER bands1, 3, 4, and 8 for Fe/Mg-OH alteration

PCs	Channel				V（%）
	ASTER1	ASTER3	ASTER4	ASTER8	
PC1	0.79427	0.59190	0.13504	0.02357	92.20%
PC2	-0.60608	0.75650	0.24419	0.02731	6.24%
PC3	-0.04151	0.27796	-0.94629	-0.15986	1.53%
PC4	-0.00893	0.00995	-0.16333	0.98648	0.03%

Table 3 Principal components from ASTER bands1, 2, 3, and 4 for Fe^{2+} and Fe^{3+} alteration

PCs	Channel				V（%）
	ASTER1	ASTER2	ASTER3	ASTER4	
PC1	0.62211	0.45532	0.10544	0.62813	93.83%
PC2	-0.45608	0.83490	0.23961	-0.19372	4.06%
PC3	-0.53225	-0.27540	0.47029	0.64784	1.31%
PC4	-0.34883	0.14065	-0.84279	0.38501	0.80%

The anomalies can be identified using an ordinary method based on mean and standard deviation of the distribution mean +n standard deviation, where n is a number determining the time of deviation from the mean value with standard deviation as the reference. We use 2 to classify the scores on PC4 as anomalies. The results are shown in Fig. 1.

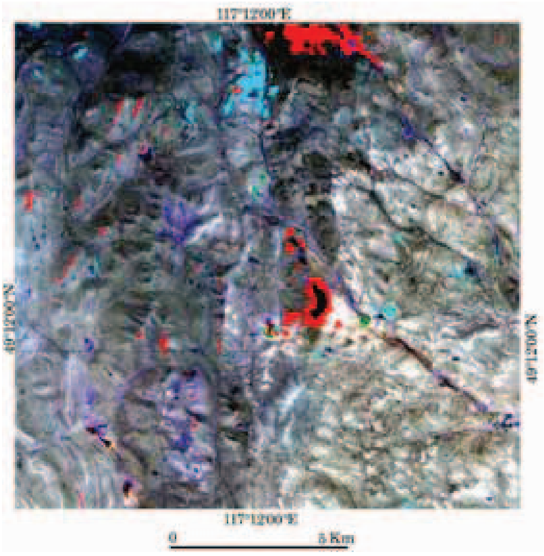

Fig.1. Alteration anomaly image, red patterns correspond to Fe ion, blue correspond to Al-OH, cyan patterns correspond to Fe/Mg-OH alteration

4. CONCLUSION

We compare the locations of 5 known mineral deposits with the patterns shown in Fig.1. All deposits are related to zones of mineral alteration obtained from remote sensing. These results may indicate that the zones of mineral alteration identified from remote sensing can be taken as targets for mineral exploration. The study shows that ASTER data may provide independent parameters useful for regional geological surveys.

5. REFERENCE

[1] H. Fujisada, F. Sakuma, A. Ono, and M. Kudoh. "Design and Preflight Performance of ASTER Instrument Protoflight Model". IEEE TRANSACTIONS ON GEOSCIENCE AND REMOTE SENSING, 36(4), 1151-1159,1998.

[2] Rowan, L. C., Mars, J. C.. "Lithologic mapping in the Mountain Pass, California area using Advanced Spaceborne Thermal Emission and Reflection Radiometer (ASTER) data". Remote Sensing of Environment 84, 350–366, 2003.

[3]Yoshiki Ninomiya, Bihong Fu, Thomas J. Cudahy. "Detecting lithology with Advanced Spaceborne Thermal Emission and Reflection Radiometer (ASTER) multispectral thermal infrared ''radiance-at-sensor'' data". Remote Sensing of Environment, 99, 127 – 139, 2005.

[4]Rowan, L. C., Mars, J. C, Colin J. Simpson. "Lithologic mapping of the Mordor, NT, Australia ultramafic complex by using the Advanced Spaceborne Thermal Emission and Reflection Radiometer (ASTER)". Remote Sensing of Environment 99, 105 -126, 2005.

[5]Goetz, A. F. H., Rock, B. N., Rowan, L. C. "Remote sensing for Exploration: An overview". Economic Geology, 78(4), 573−590. 1983.

[6]Ranjbar,H., Honarmand, M., Moezifar, Z., 2004. Application of the Crosta Technique for Porphyry Copper Alteration Mapping Using ETM+ Data in the Southern Part of the Iranian Volcanic Sedimentary Belt, Journal of Asian EarthSciences, 24:237-243.